

Supporting Information for

Microstructure Analysis of Biocompatible Phosphoester-*co*-polymers

Tobias Steinbach,^{a,b,c} Romina Schröder,^a Sandra Ritz,^c Frederik R. Wurm^c

^a*Institute of Organic Chemistry, Johannes Gutenberg-University (JGU), Duesbergweg 10-14,
55099 Mainz, Germany*

^b*Graduate School Material Science in Mainz, Staudinger Weg 9, D-55128 Mainz, Germany*

^c*Max Planck Institut für Polymerforschung, Ackermannweg 10, 55128 Mainz, wurm@mpip-
mainz.mpg.de*

Contact address: wurm@mpip-mainz.mpg.de, phone: 0049 6131 379 723, fax: 0049 6131 370

330.

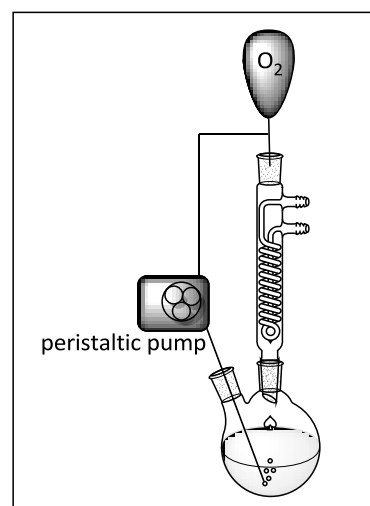
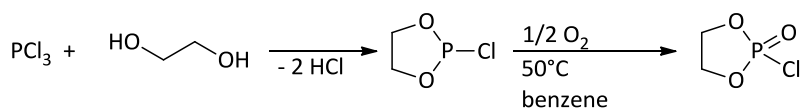


Fig. S1. Experimental setup for the oxidation of 2-chloro-1,3,2-dioxaphospholane.

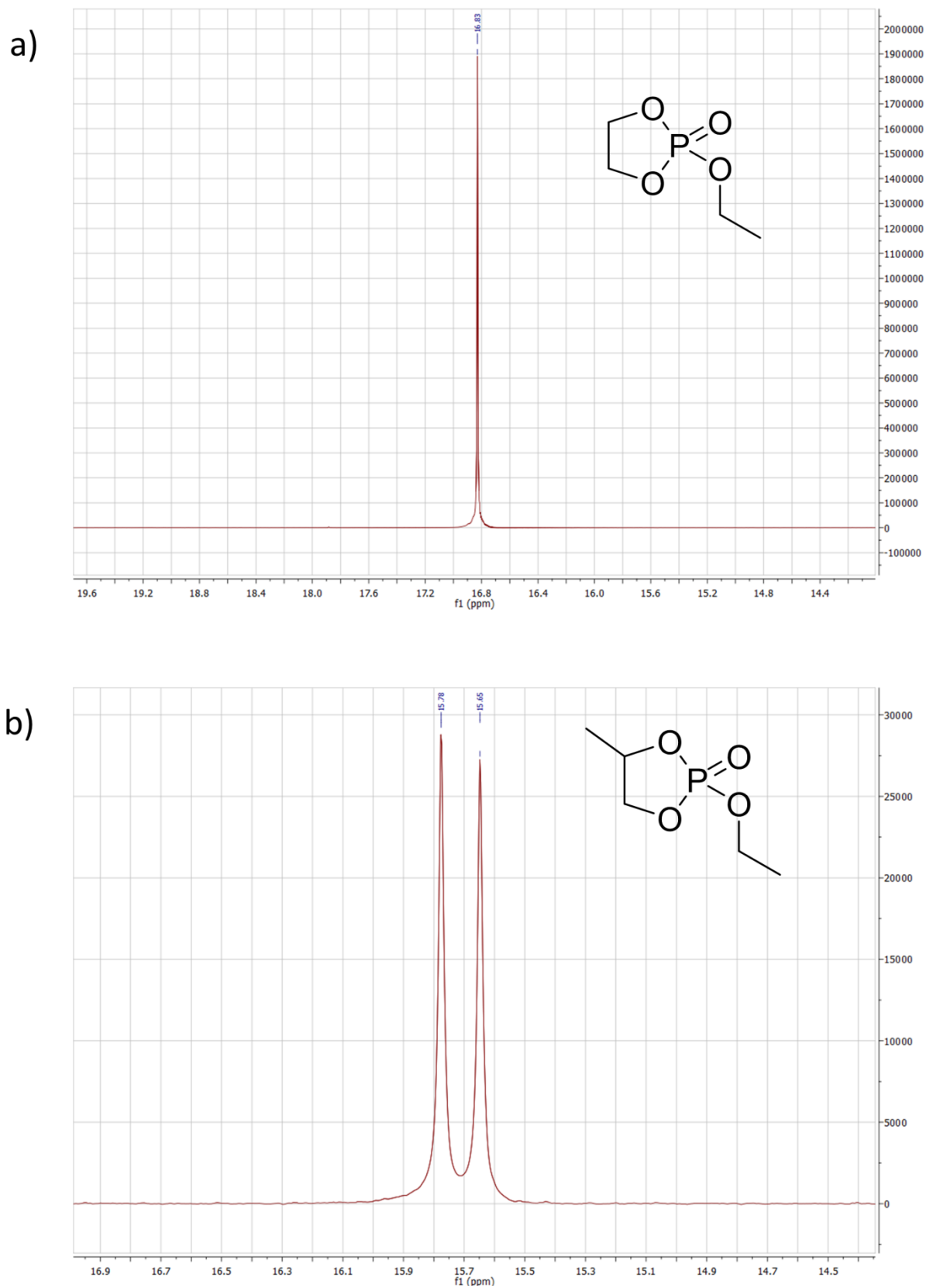


Fig. S2. ^{31}P NMR spectrum of a) EEP and b) EMEP in $\text{DMSO}-d_6$.

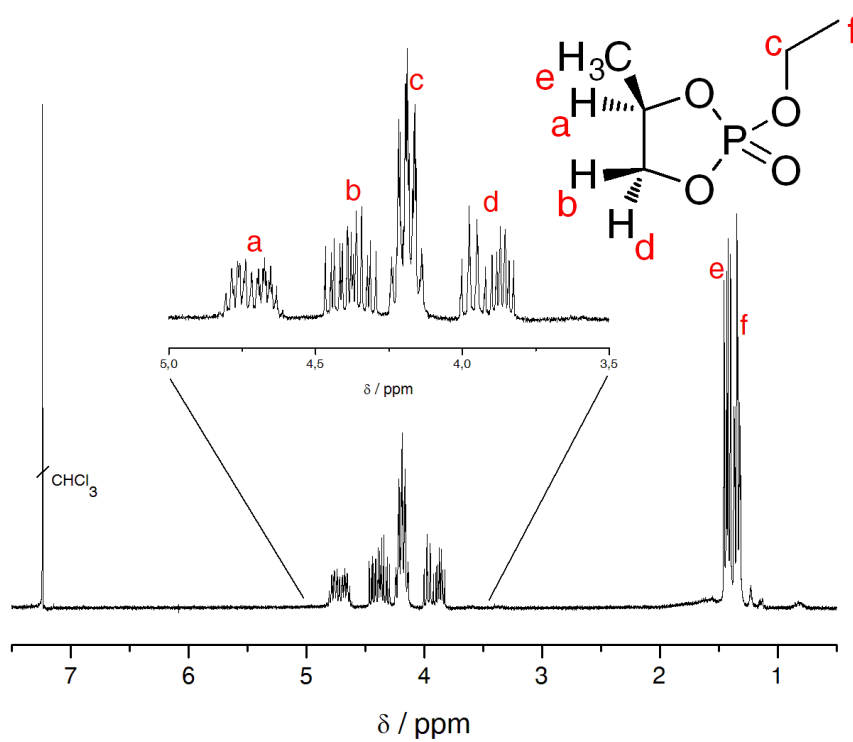


Fig. S3. ^1H NMR spectrum of EMEP in CDCl_3 .

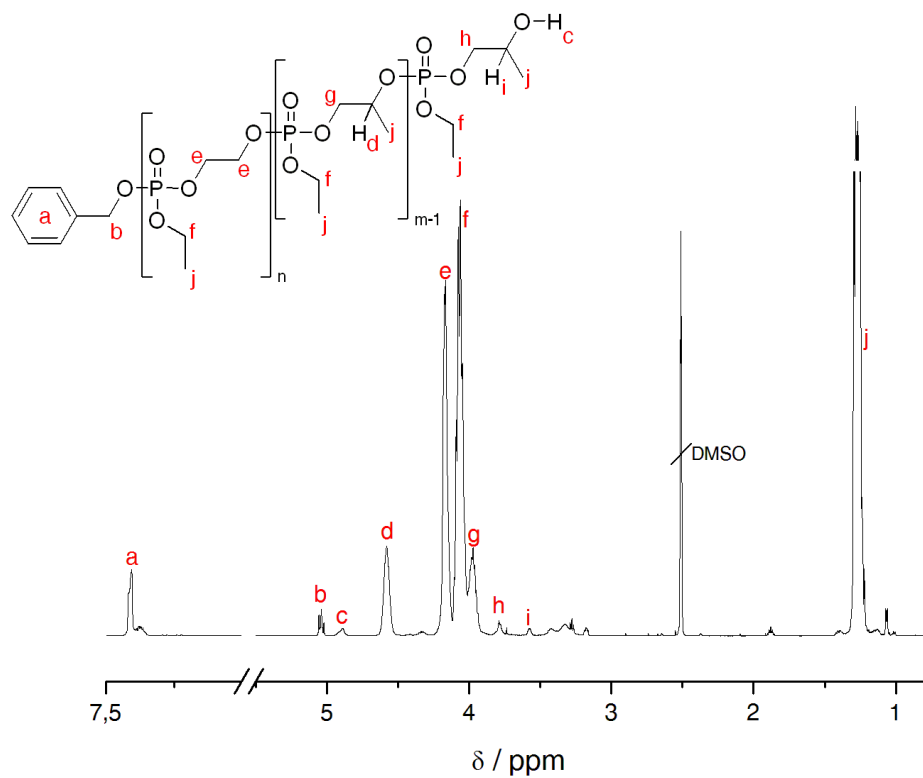


Fig. S4. ^1H NMR spectrum of P(EEP₁₇-co-EMEP₁₆) in DMSO- d_6 .

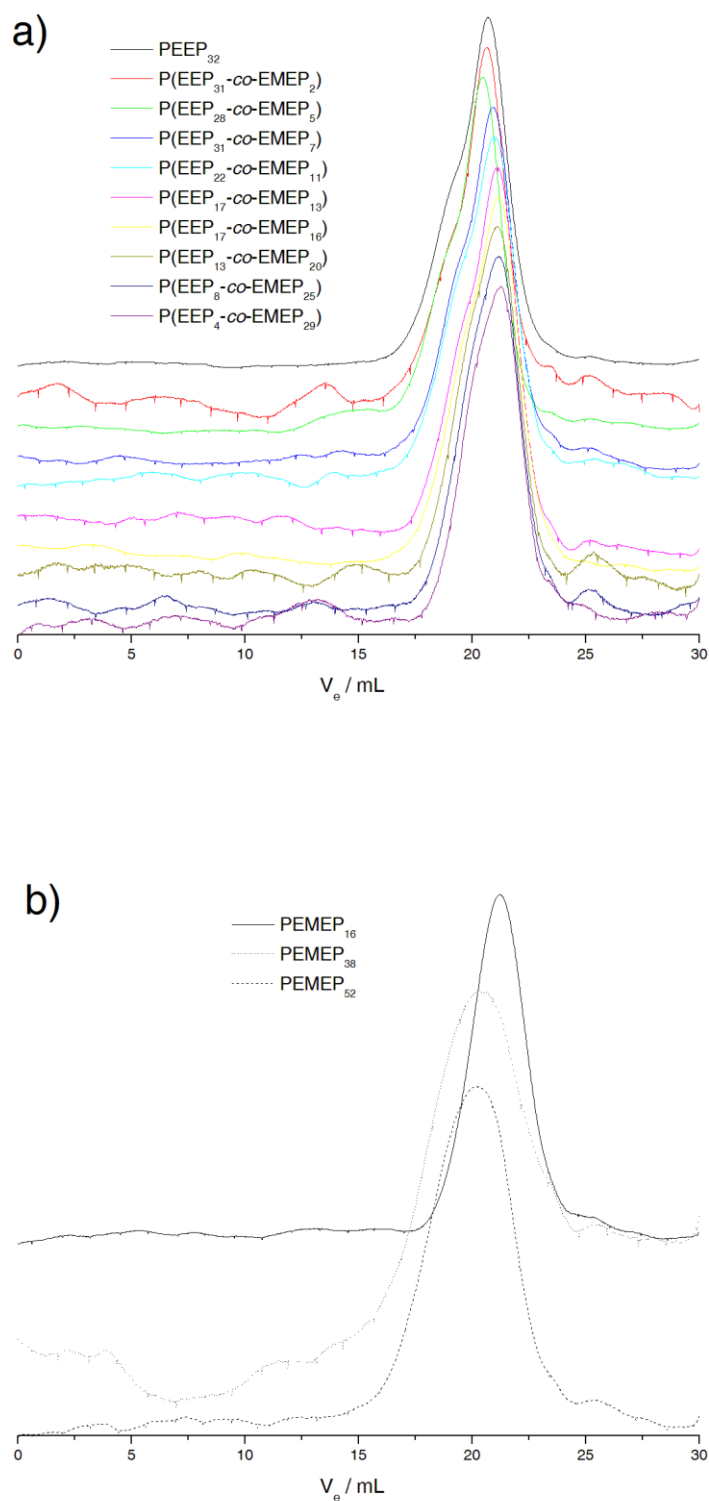


Fig. S5. SEC chromatograms of a) P(EEP-co-EMEP) copolymers and b) PEMEP homopolymers (measured in DMF at 50 °C and a flow rate of 1.0 mL·min⁻¹). Periodic artifacts are due to highly diluted samples (1.0 mg·mL⁻¹, 100 μL injected) and the high measuring sensitivity of the employed RI detector.

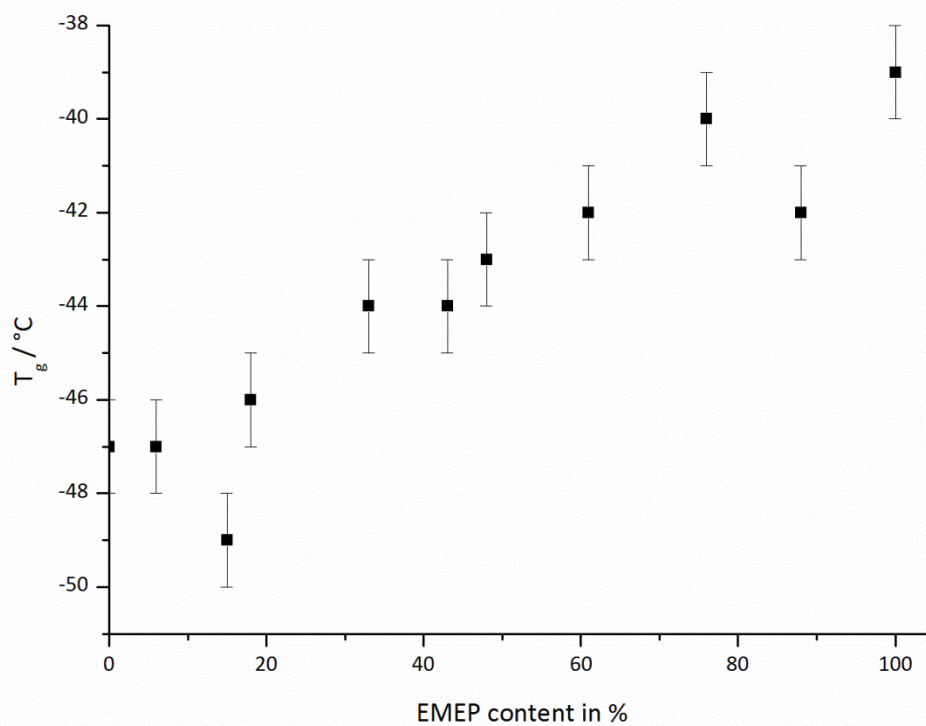


Fig. S6. Graphical representation of the measured T_g of all copolymers.

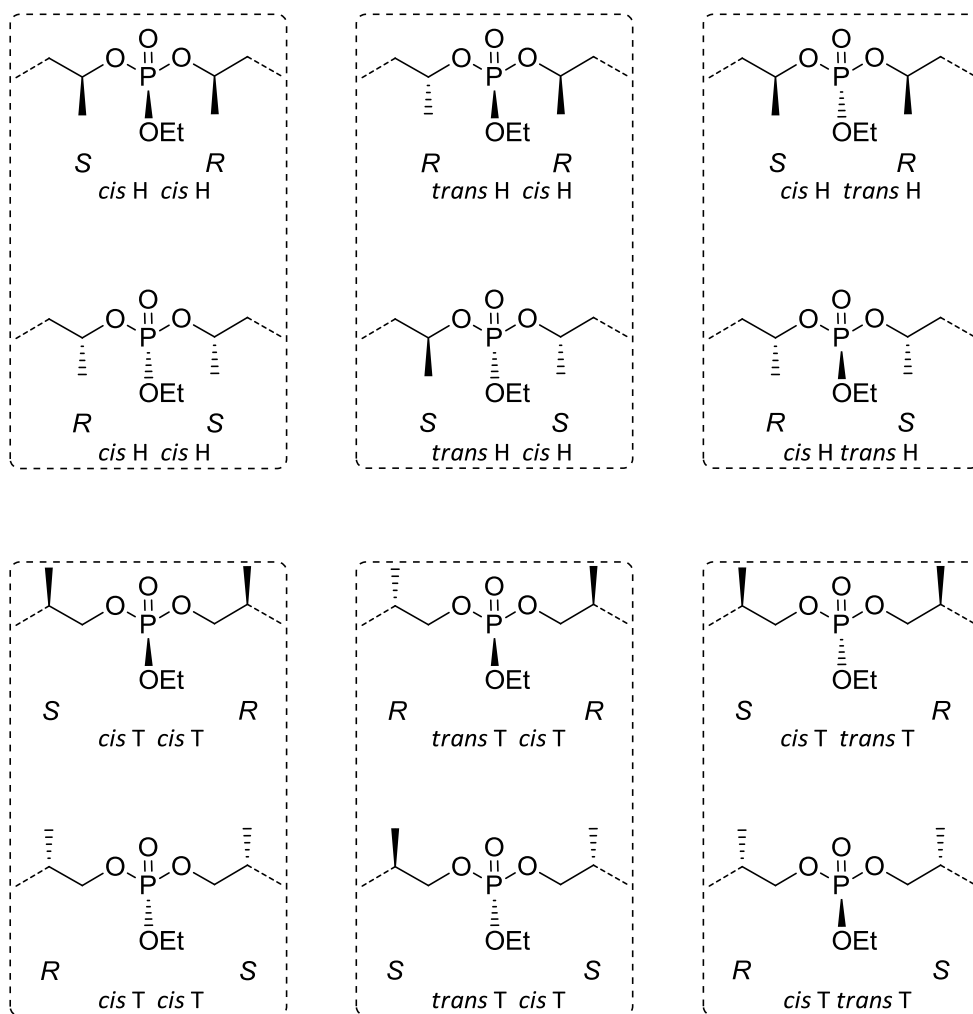


Fig. S7. Dyad analysis with all possible head-to-head (above) and tail-to-tail (bottom) configurations of PEMEP.

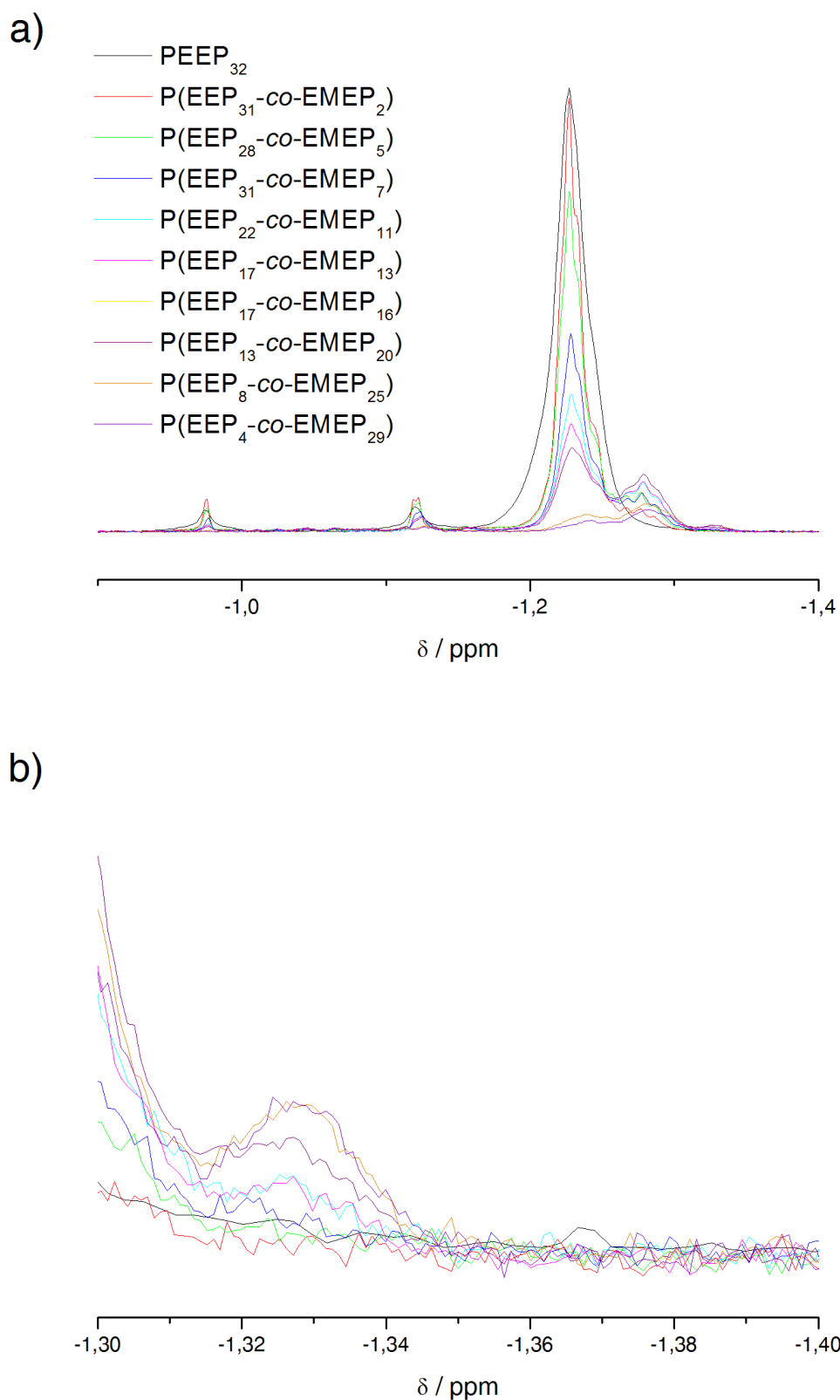


Fig. S8. ^{31}P NMR of all copolymers. a) Magnification of the tail-to-tail region. b) Zoom in the region assigned to the $\text{EMEP}_\alpha\text{-EMEP}_\beta$ dyad.

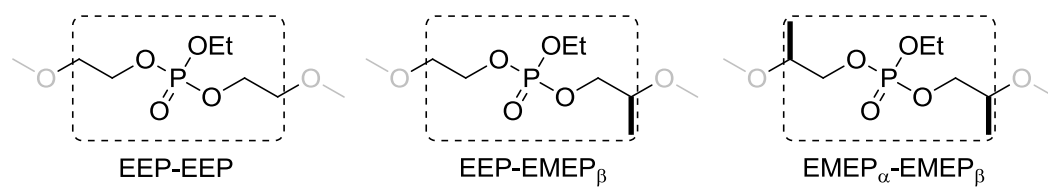
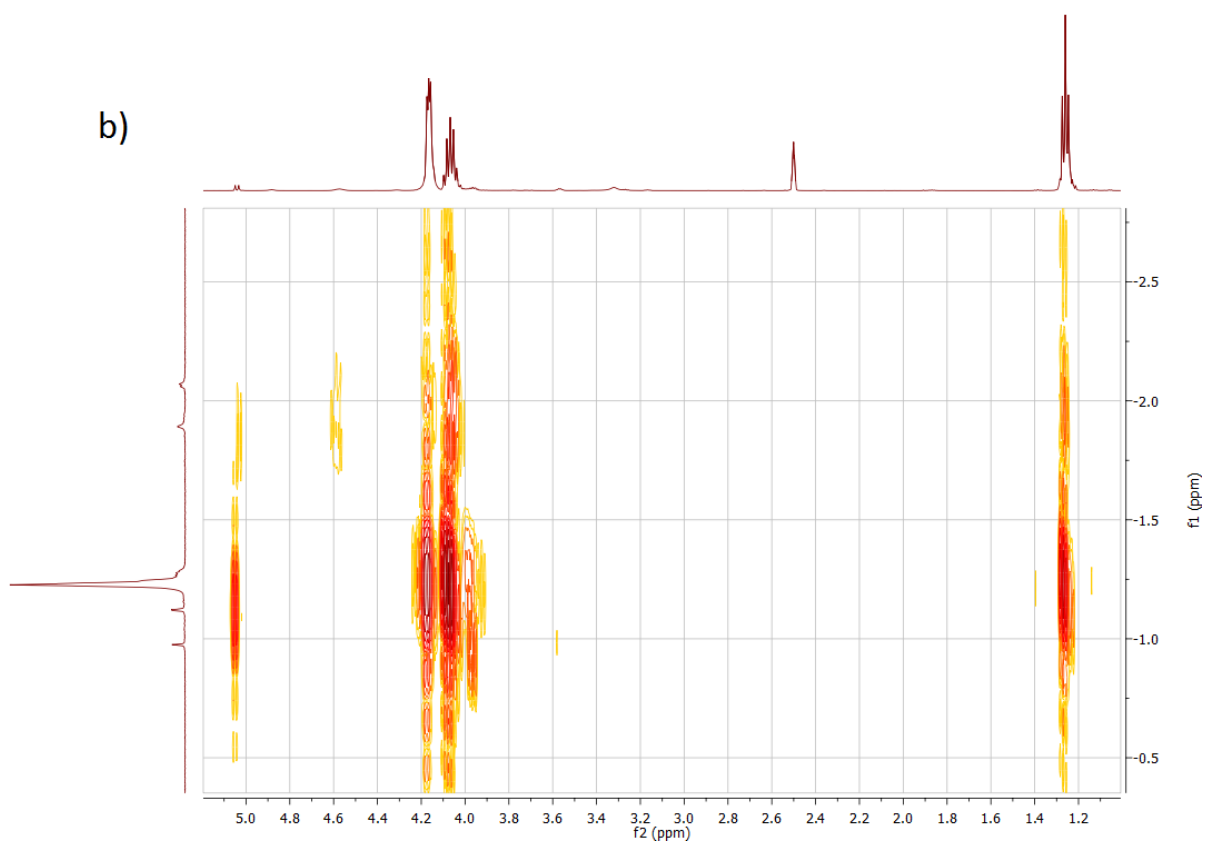
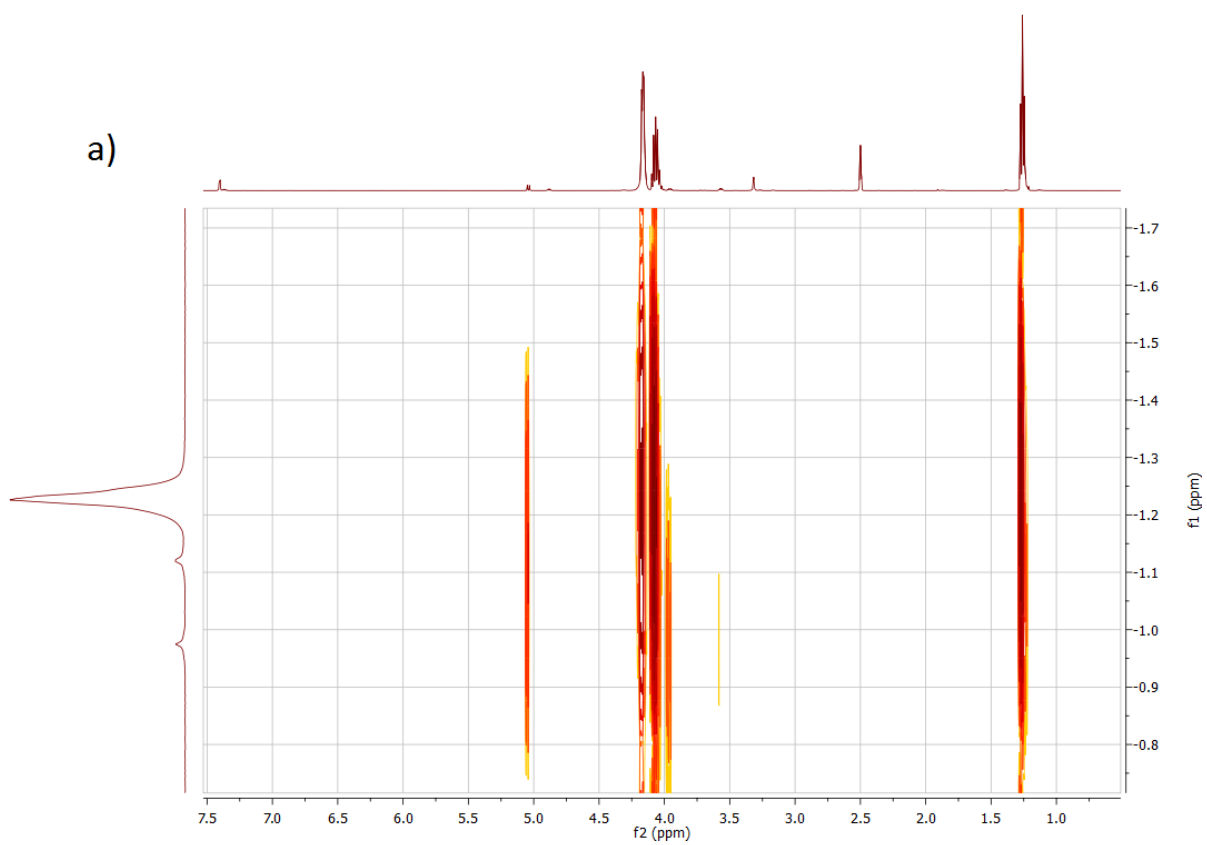
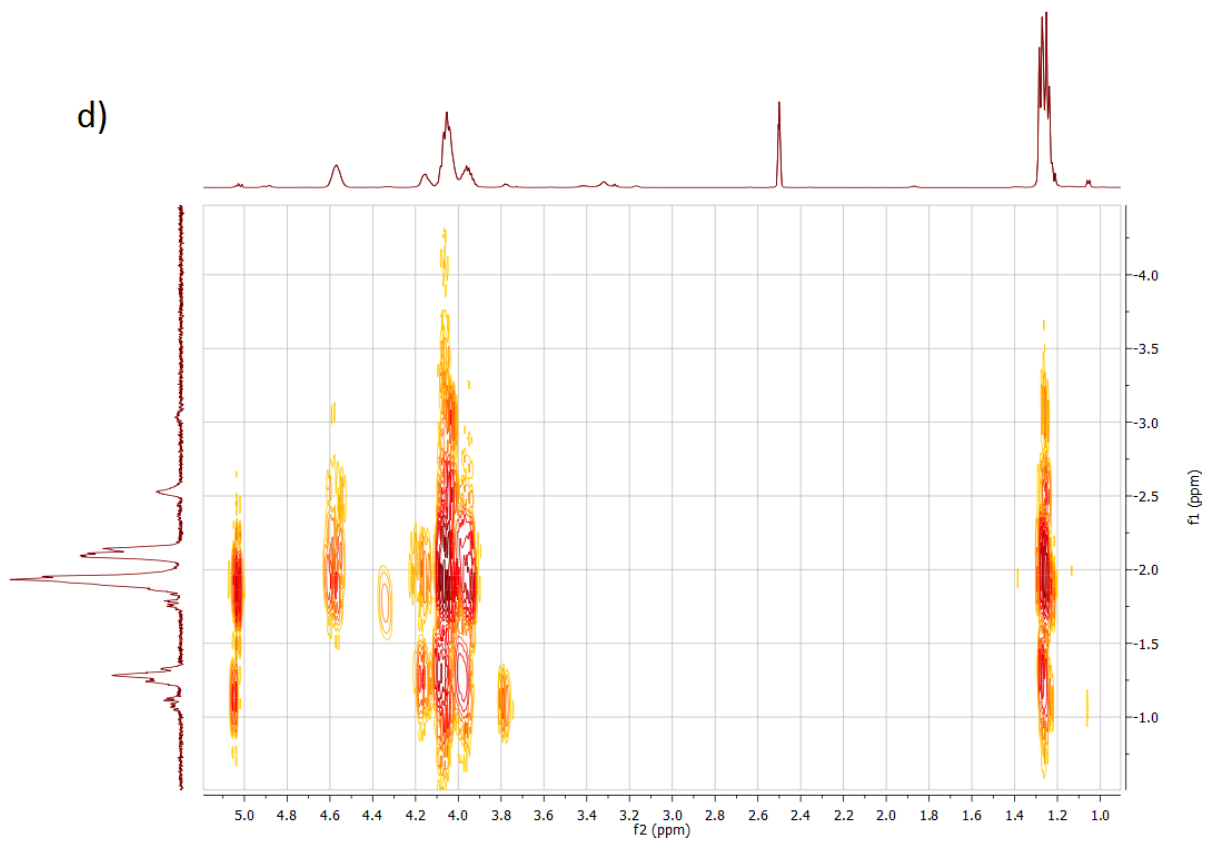
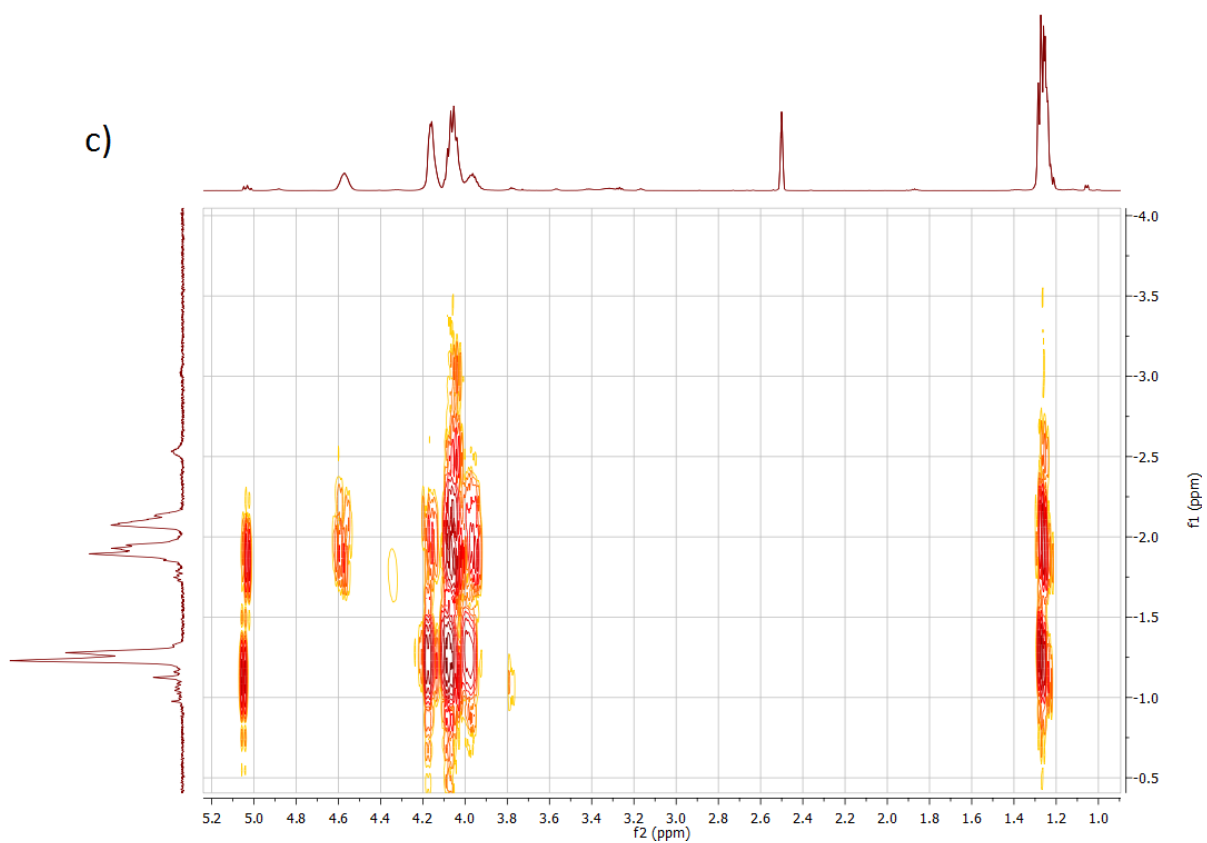


Fig. S9. Tail-to-tail microstructures resulting in different chemical shifts in ³¹P NMR (compare to Fig. S8, ESI)





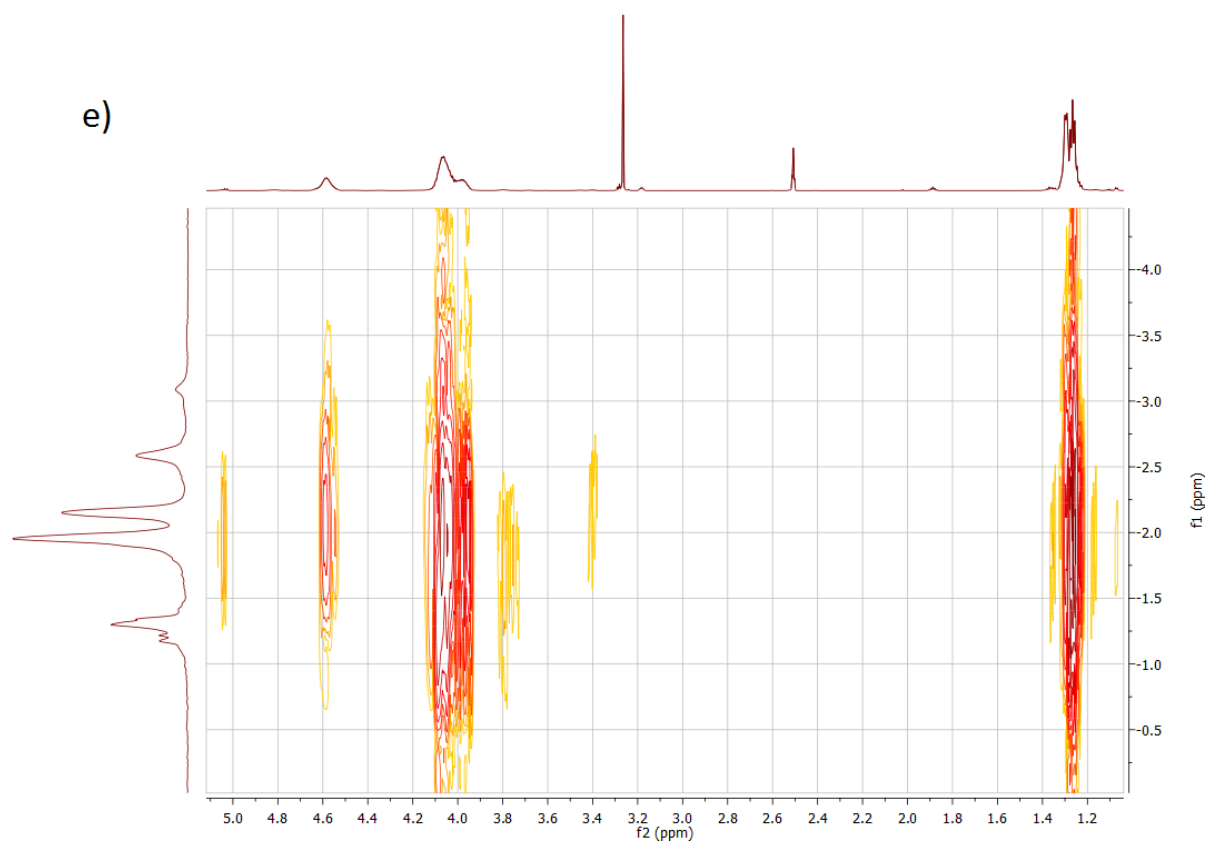
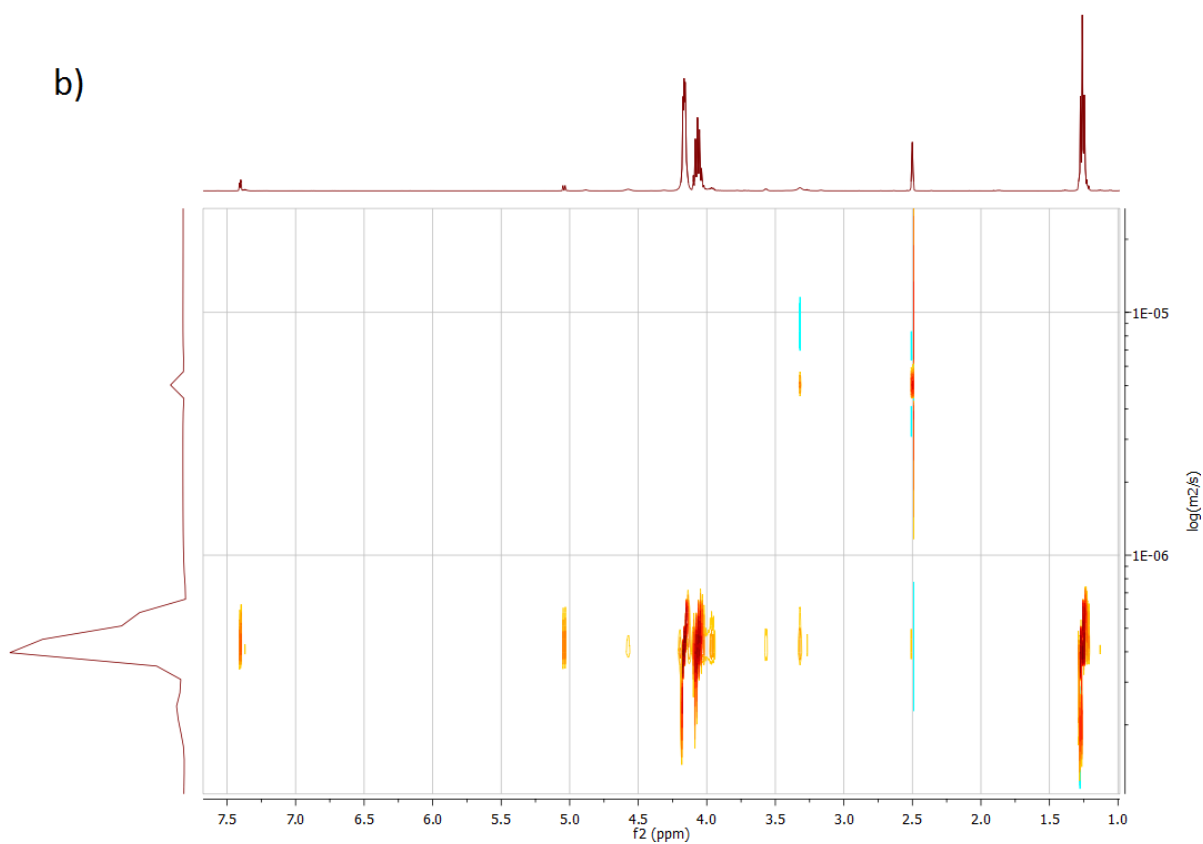
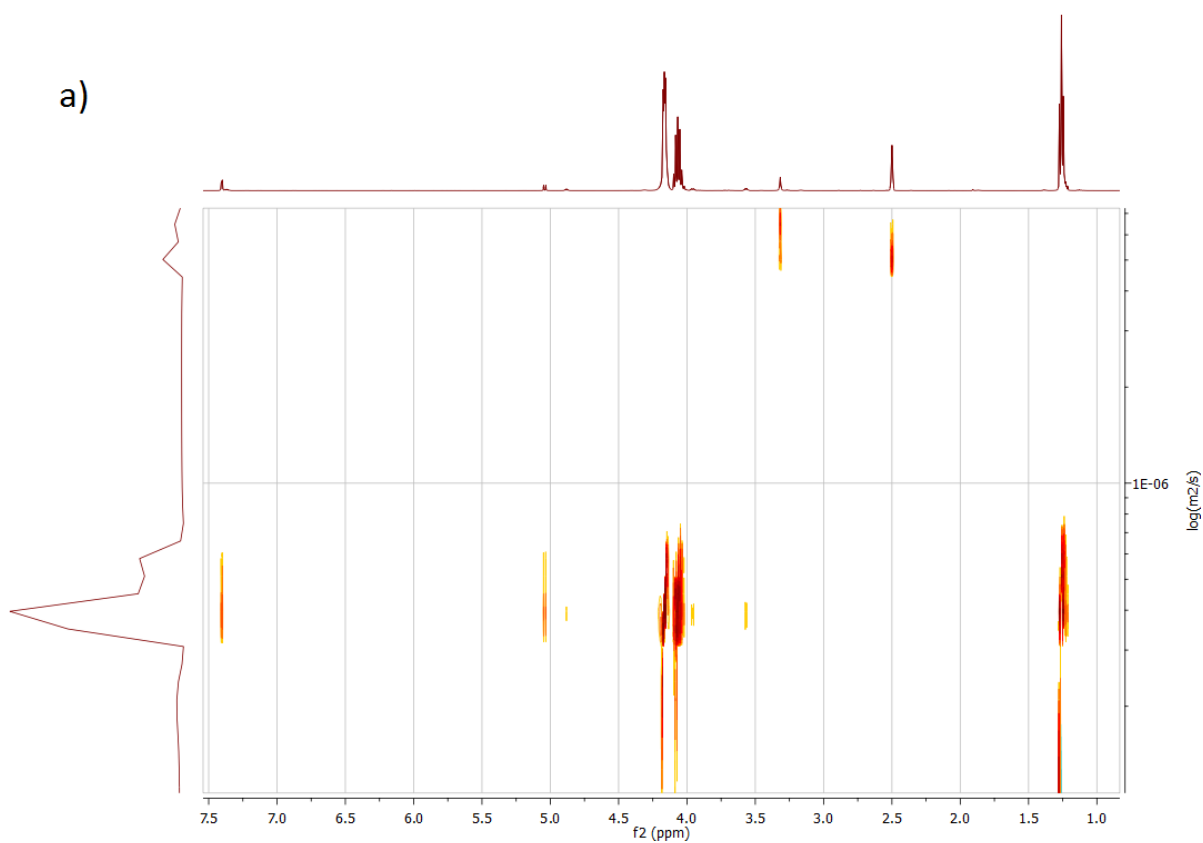
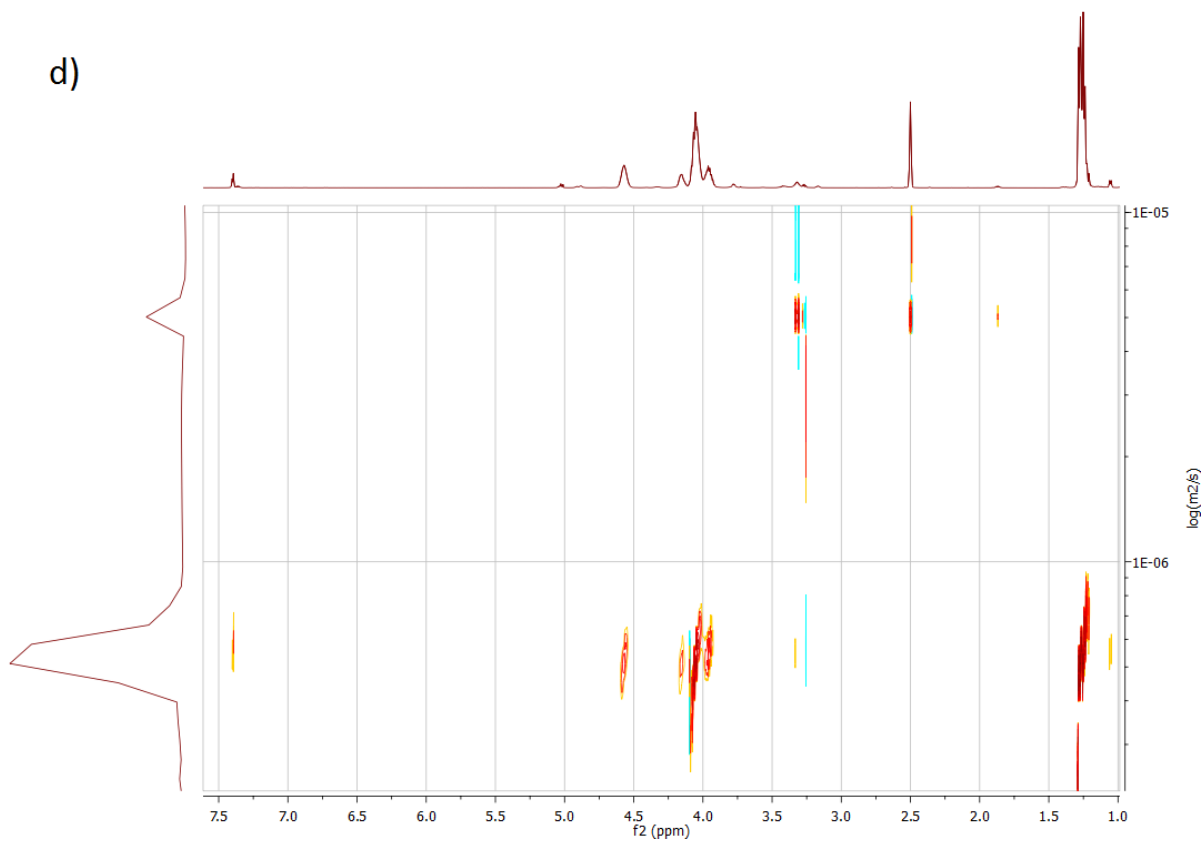
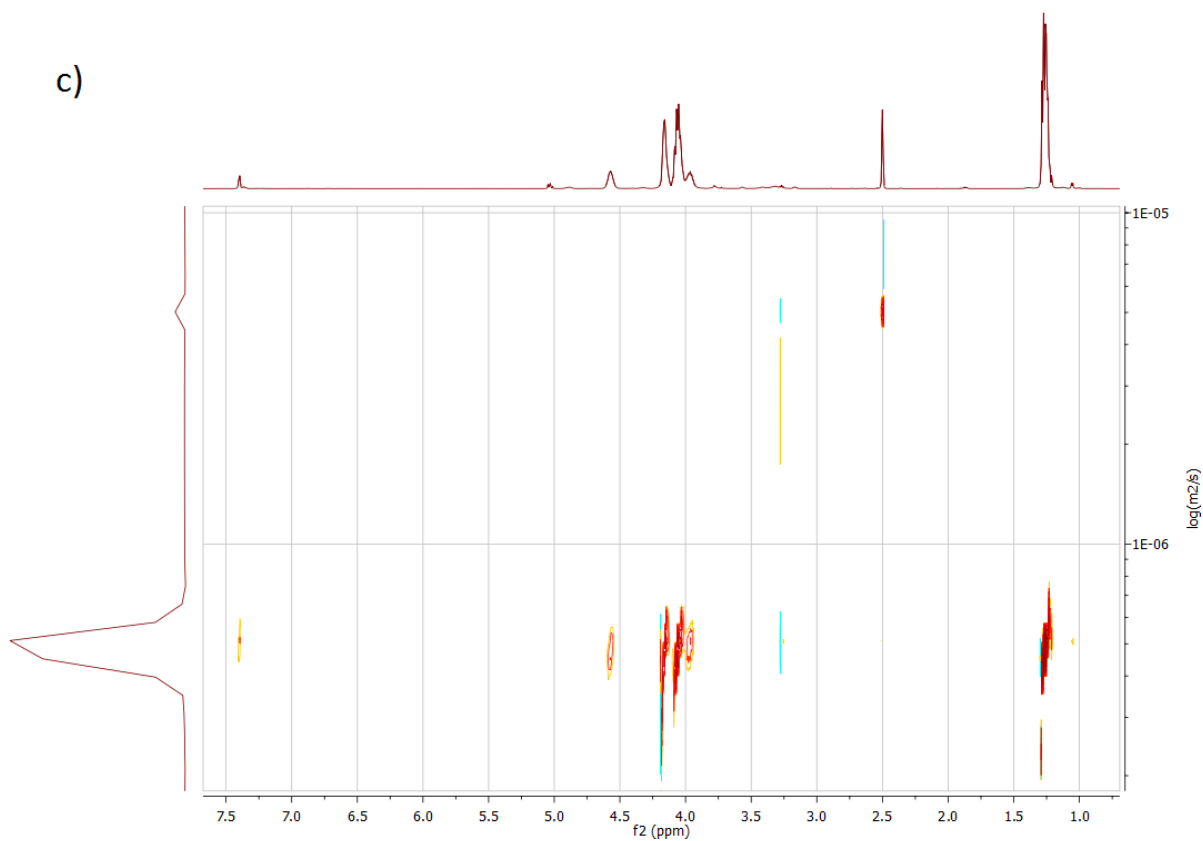


Fig. S10. ^1H - ^{31}P HMBC spectra of five representative examples in $\text{DMSO-}d_6$: a) PEEP_{32} , b) $\text{P}(\text{EEP}_{28}\text{-}co\text{-EMEP}_5)$; c) $\text{P}(\text{EEP}_{17}\text{-}co\text{-EMEP}_{16})$; d) $\text{P}(\text{EEP}_4\text{-}co\text{-EMEP}_{29})$; e) PEMEP_{38} .





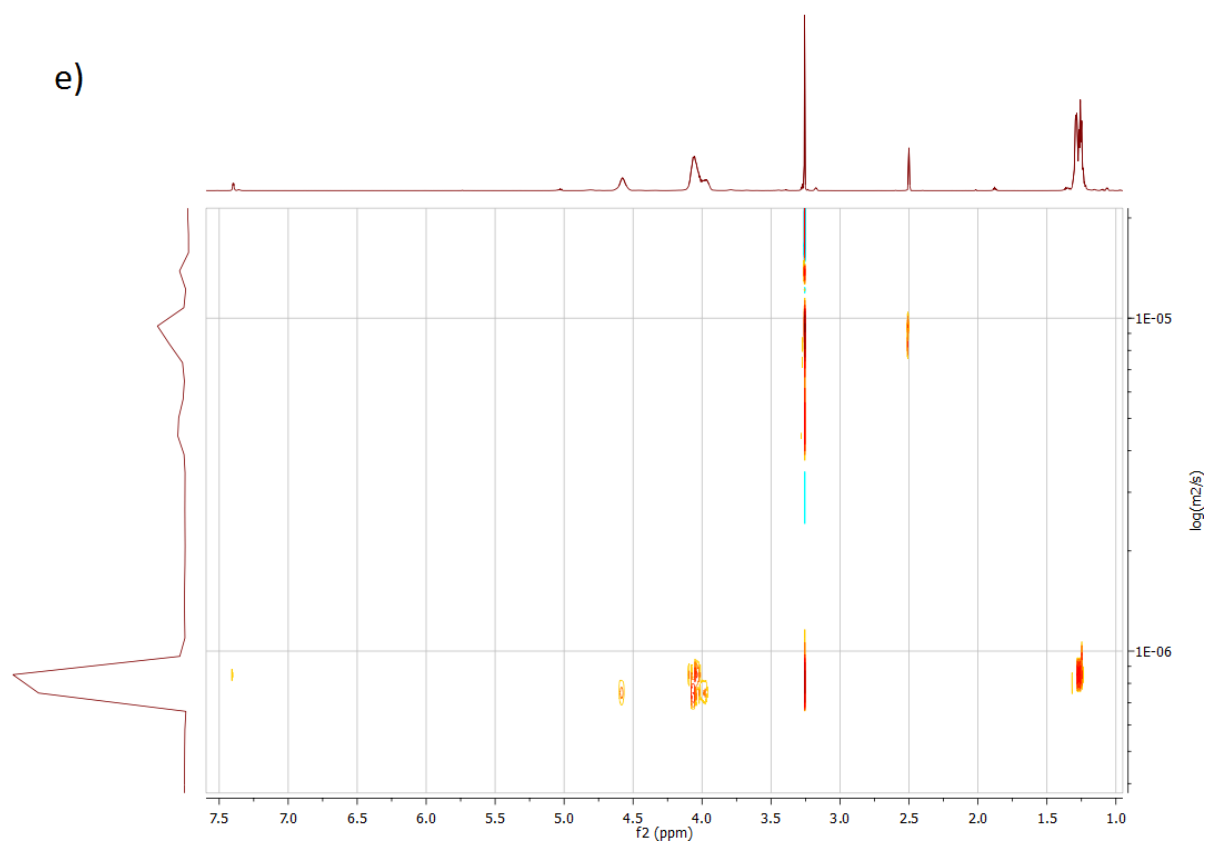


Fig. S11. ^1H DOSY of five representative examples in $\text{DMSO-}d_6$: a) PEEP_{32} , b) $\text{P}(\text{EEP}_{28}\text{-co-EMEP}_5)$; c) $\text{P}(\text{EEP}_{17}\text{-co-EMEP}_{16})$; d) $\text{P}(\text{EEP}_4\text{-co-EMEP}_{29})$; e) PEMEP_{38} . The diffusion coefficient calculated by Bayesian DOSY Transformation is for all copolymers in the same range.

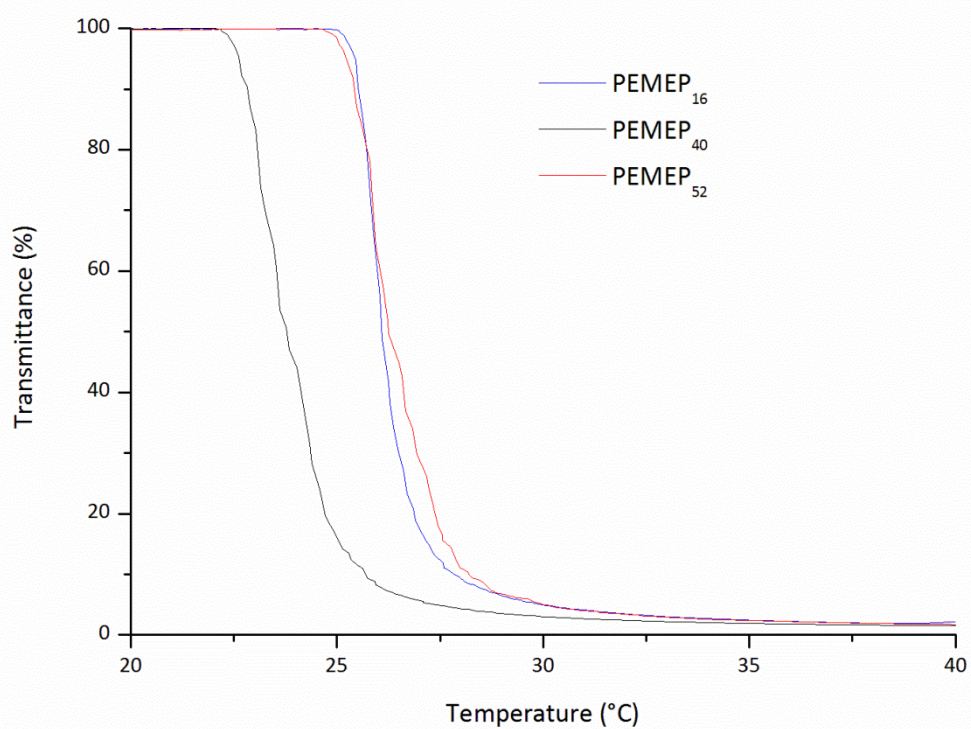


Fig. S12. Change in transmittance of PEMEP solutions with different molecular weights. Cloud points were determined in PBS pH 7.4 (10 mM) prepared from MilliQ water (18.2 mΩ) at a concentration of 10.0 mg·mL⁻¹. The heating/cooling rate was 1 °C·min⁻¹ and values were recorded every 0.1 °C.

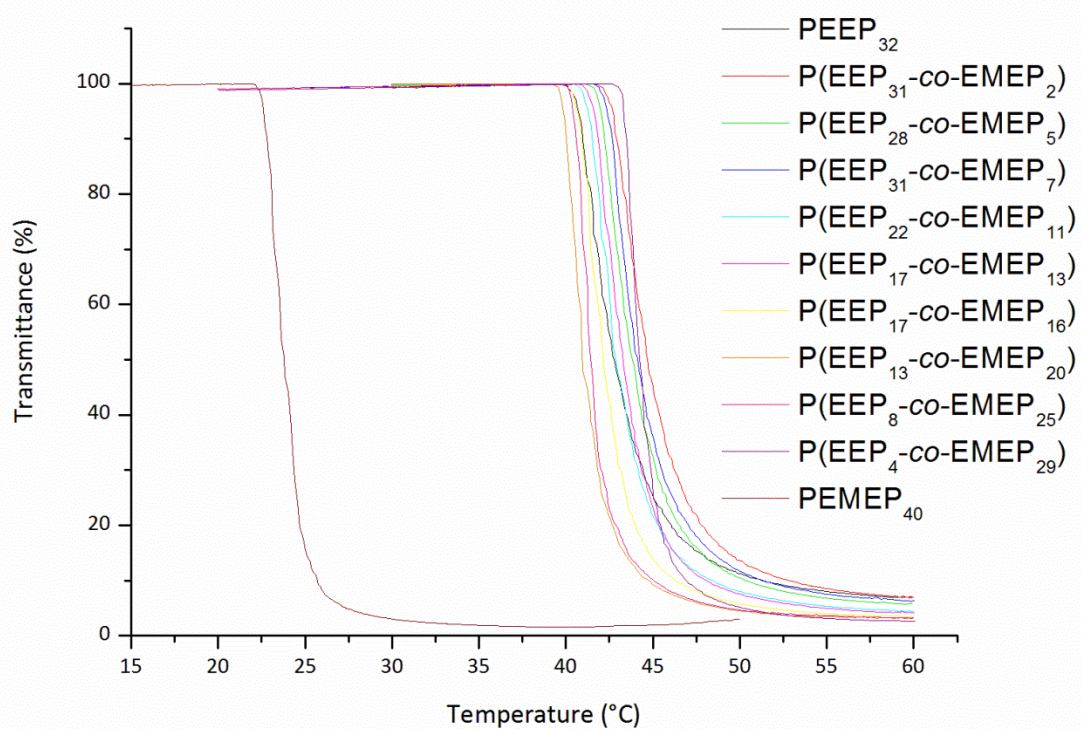


Fig. S13. Change in transmittance of P(EEP-co-EMEP) copolymers at a concentration of 10 $\text{mg}\cdot\text{mL}^{-1}$ in PBS pH 7.4 10 mM at 500 nm and a heating rate of $1^\circ\text{C}\cdot\text{min}^{-1}$.